Rapid Communications

Resonant nonlinear refraction of 4.3-μm light in CO_2 gas

J. J. Pigeon,[1,*] D. Tovey,[2] S. Ya. Tochitsky,[2] G. J. Louwrens,[2] I. Ben-Zvi,[1] D. Martyshkin,[3] V. Fedorov,[3] K. Karki,[3] S. Mirov,[3] and C. Joshi[2]

[1]*Department of Physics and Astronomy, Stony Brook University, Stony Brook, New York 11794, USA*
[2]*Department of Electrical Engineering, University of California at Los Angeles, Los Angeles, California 90095, USA*
[3]*Department of Physics, University of Alabama at Birmingham, Birmingham, Alabama 35294, USA*

(Received 24 April 2019; published 30 July 2019)

We use time- and frequency-resolved measurements of self-focusing and self-defocusing of 4.3-μm radiation in CO_2 gas to study the resonant nonlinear optical response in the vicinity of individual rovibrational lines. Measurements over a range of lines on the 4*P* and 4*R* branch of the 000-001 transition indicate that the nonlinear response of CO_2 is strongly affected by power broadening, resulting in a sign reversal of the nonlinearity as compared to that of a saturable two-level system.

DOI: 10.1103/PhysRevA.100.011803

I. INTRODUCTION

The resonant interaction of light with matter is the central pillar of atomic, molecular, and optical physics. Moreover, knowledge of the resonant nonlinear optical response of atoms and molecules in the gas phase underpins the progress of a wide range of subfields such as nonlinear optics, quantum electronics, and ultrafast science. With the advent of spectrally bright and coherent laser sources, there have been extensive theoretical and experimental studies dedicated to understanding the resonant nonlinear optical interaction of visible and near-IR light with the electronic transitions of atomic gases, usually alkali-metal vapors. In doing so, researchers have observed and characterized numerous resonant optical phenomena such as saturable absorption [1], resonant self-focusing [2], self-defocusing [3], electromagnetically induced transparency [4], and the production of slow light [5]. Further sophistication of this effort has even enabled single-photon nonlinear processes, thus providing a notable advance in the field of quantum optics [6].

There has been much less effort, however, dedicated to performing such experiments in molecular gases, where the nonlinear optical effects are dominated by rovibrational transitions that are active in the mid- and long-wave IR (LWIR) spectral range. These studies, hindered by a lack of high-power, continuously tunable sources in the LWIR, have been performed using line-tunable CO_2 lasers, thereby constraining measurements to a coincidental overlap between CO_2 laser lines and the transitions of molecules under investigation. As a result, previous studies on nonlinear self-focusing and self-defocusing have been limited to molecules such as SF_6, NH_3, and CDF_3 [7–11] for which the spectra are rather complicated. Both basic and applied research in this field would benefit from extending these studies to smaller molecules such as CO_2 and CO that have fewer modes of vibration. Thus, their relatively simple spectra allow for a systematic study of the resonant nonlinear optical response in the vicinity of individual rovibrational lines. Furthermore, these molecules exist in substantial quantities in the atmosphere and, as a result, measurements of the nonlinear rovibrational response of such IR-active, minor air constituents are needed to support the burgeoning interest in the LWIR filamentation in air [12] and in the development of a nonlinear refractive index equivalent of the HITRAN database [13].

In this Rapid Communication, we report a study of the resonant rovibrational nonlinearity of CO_2 gas driven by a continuously tunable, Fe:ZnSe laser operating near 4.3 μm. By performing frequency- and time-resolved measurements of self-focusing and self-defocusing of the 4.3-μm beam, we have characterized the dispersion of the resonant Kerr nonlinearity in the vicinity of a single rovibrational line of the CO_2 molecule. We have found that the rovibrational nonlinearity of CO_2 is dominated by the resonant ac-Stark or power broadening effect and that the sign of the nonlinearity is opposite to that predicted by the commonly used two-level system model that describes the resonant nonlinear optics of both atoms and molecules in the gas phase [14]. We determine that the nonlinear refractive index of low-pressure CO_2 is $\sim 10^{-12}$ cm^2/W, suggesting that the 400-ppm CO_2 concentration can act to increase the nonlinear refractive index of ambient air by four orders of magnitude as compared to the nonresonant values measured in the mid- and LWIR [15–18].

II. EXPERIMENT

Continuously tunable mid-IR laser pulses produced by a Fe:ZnSe laser system were used to study the resonant nonlinear optics of CO_2 gas. The room-temperature Fe:ZnSe laser was optically pumped by 2.94-μm, 15-mJ laser pulses produced by a *Q*-switched Er:yttrium aluminum garnet (YAG) oscillator to generate 2-mJ, 40-ns laser pulses at 10 Hz, tunable in the range 3.6–5.1 μm [19]. Figure 1 depicts a simplified experimental setup. We focused the 4.3-μm beam to a full width at half maximum (FWHM) beam diameter of $\sim$600 μm, resulting in a peak intensity of $\sim$15 MW/cm^2 at

*jeremy.pigeon@stonybrook.edu

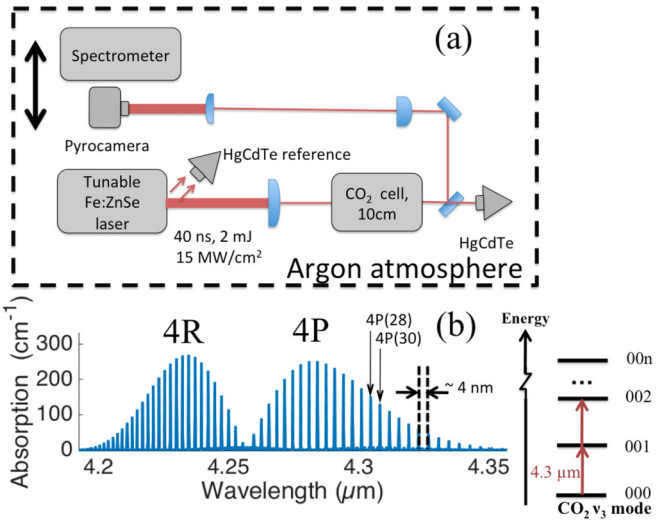

FIG. 1. (a) Simplified experimental setup used for measurements of resonant self-focusing and self-defocusing of 4.3-μm light in CO_2 gas and (b) absorption spectrum of CO_2 (100 Torr, 295 K) obtained from the HITRAN database showing the rovibrational structure of the so-called 4*R* and 4*P* branches [13]. The inset is a simplified energy-level diagram of CO_2 showing only the 4.3-μm 000-00*n* (ν_3) vibrational asymmetric stretching mode.

the entrance of the gas-filled cell. After propagating through the 10-cm-long cell, the beam was split by a 50/50 beam splitter to perform simultaneous temporal and spatial measurements. The exit of the cell was imaged and magnified by a factor of 5 using a telescope and measured with a pyroelectric camera. Frequency-resolved measurements of self-focusing and self-defocusing were performed using a spectrometer with the pyrocamera as a readout device. The resolution of the spectrometer is <1 nm. It should be noted that the FWHM of the Fe:ZnSe laser bandwidth is <2 nm and that the spacing between rovibrational lines of the 4*P* branch of the CO_2 molecule [see Fig. 1(b)] is $\sim$4 nm. As a result, the laser spectrum only interacts with an individual line on the long-wavelength side of the CO_2 absorption spectrum (4*P* branch) where the line spacing is the greatest. The entire experimental setup was purged with argon to avoid absorption related to CO_2 in the air.

III. RESULTS

We have observed a self-focusing, self-defocusing, and transverse beam breakup indicative of multiple filamentation after propagating the 4.3-μm laser pulses tuned to various spectral locations within the 4*P* branch of pure CO_2. Figure 2 shows typical two-dimensional beam profiles that demonstrate these physical effects and were measured in $\sim$50 Torr of CO_2. Figure 2(a) shows the initial beam profile, measured when the cell was evacuated. Note that for the self-focusing and self-defocusing cases [Figs. 2(b) and 2(c), respectively], the laser was tuned in the vicinity of a rovibrational line on the long-wavelength wing of the 4*P* branch. The beam profile showing a transverse beam breakup [Fig. 2(d)] was observed for a case when the laser was tuned to the self-focusing side of a rovibrational line near the peak of the 4*P* branch. A typical absorption was measured to be between

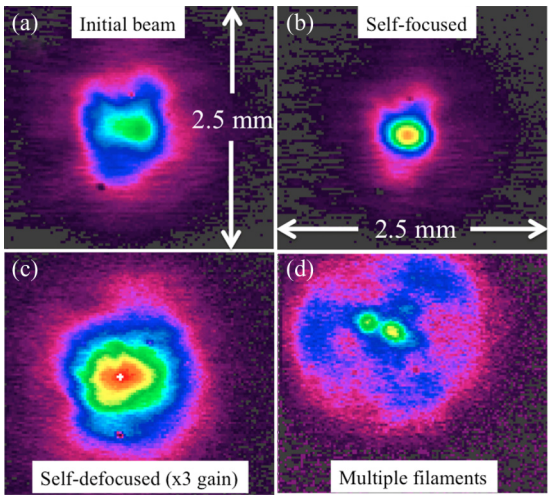

FIG. 2. (a) Initial 4.3-μm beam profile and beam profiles for a case when the laser was tuned to the (b) self-focusing and (c) self-defocusing sides of a rovibrational line located on the wing of the 000-001 4*P* branch of CO_2. (d) Beam profile showing transverse beam breakup indicative of multiple filamentation for a case when the laser was tuned to the self-focusing side of a rovibrational line near the peak of the 4*P* branch.

30% and 70% depending on CO_2 pressure and the laser wavelength, resulting in an absorbed energy of 0.6–1.4 mJ.

To characterize the spatial changes to the beam caused by nonlinear focusing we have measured the evolution of the beam profile with variable pressure. Figure 3 is a plot of the FWHM beam diameter as a function of cell pressure for a case when the laser was tuned to the self-focusing and self-defocusing sides of resonance. As can be seen in Fig. 3, the FWHM beam diameter decreased from $\sim$600 to 200 μm for the self-focusing case and increased to $\sim$800 μm for the self-defocusing case when the pressure was varied from 0 to 100 Torr.

To determine the sign of the nonlinear refractive index on either side of the resonance we performed frequency-resolved measurements of nonlinear focusing. Figure 4 shows

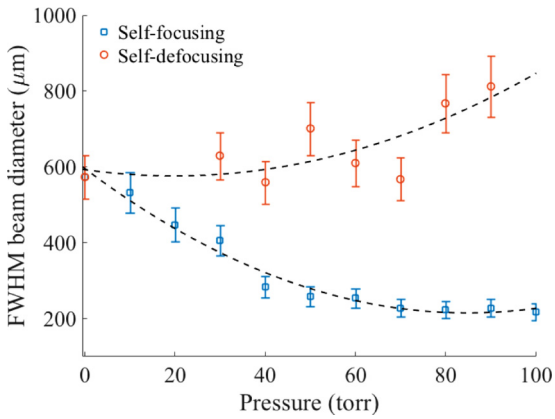

FIG. 3. The evolution of the FWHM beam profile as a function of CO_2 pressure for a case when the laser was tuned to the self-focusing (blue squares) and self-defocusing (orange circles) sides of resonance. The dashed lines are quadratic fits to the data intended to guide the eye.

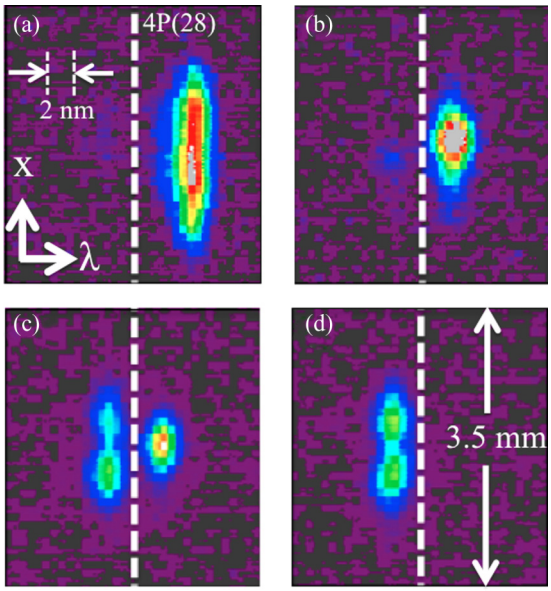

FIG. 4. Frequency-resolved measurements of self-focusing and self-defocusing in the vicinity of a rovibrational line of the 000-001 transition of CO_2. (a) shows the unaffected beam where the location of the line is marked by the vertical dashed line. (b) shows the beam self-focusing as the rovibrational line is approached from the red side of resonance. (c) shows the laser spectrum both focusing and defocusing on either side of resonance. (d) shows the laser defocusing on the blue side of resonance. It should be noted that the dumbbell shape is the one-dimensional cross section of the doughnut-shaped beam that is produced from self-defocusing and that the elongated beam profiles result from imaging the slit of the spectrometer.

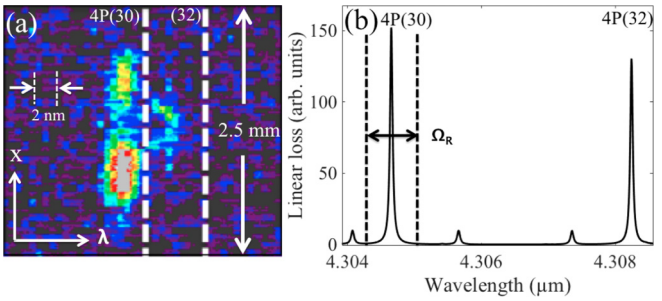

FIG. 5. (a) Frequency-resolved self-focusing measurement showing apparent power broadening of the $4P(30)$ line of CO_2. The field dependence of the Rabi frequency gives rise to a ring-shaped intensity distribution since the maximum shift is on axis where the laser intensity is maximum. (b) The absorption spectrum of CO_2 in the vicinity of the $4P(30)$ and $4P(32)$ line from the HITRAN database with a depiction of the level splitting that may be achieved based on the calculated Rabi frequency.

the results of these measurements for a case when the laser spectrum was tuned around the $4P(28)$ (∼4301-nm) line of the 000-001 transition of CO_2. The pyrocamera images presented in Fig. 4 represent wavelength versus space plots. Here, the location of the rovibrational line is denoted with a dashed white line. Note that the location of the line was identified by observing the attenuation of the blue wing of the laser's spectrum and is an estimate to within 1 nm of the location of the resonance at low laser intensity. Figure 4(a) depicts the unaffected beam detuned from the rovibrational line. As can be seen in Fig. 4(b), the laser beam begins to focus as the rovibrational line is approached from the red side of resonance. Figure 4(c) shows the beam focusing and defocusing on either side of the resonance since the $4P(28)$ line is in the middle of the laser bandwidth. Finally, Fig. 4(d) shows that the beam is defocused on the blue side of the rovibrational line. It should be noted that the dumbbell shape visible in Fig. 4(d) is the cross section of the doughnut-shaped beam that is produced by strong self-defocusing. This doughnut shape has also been observed in early experiments on self-defocusing in Rb vapor [3]. These measurements indicate that the sign of the nonlinearity around the individual rovibrational lines of CO_2 is opposite to what has been observed in other atomic and molecular gases and that predicted by the two-level model developed by Javan and Kelley [14]. The potential origin of this sign reversal is discussed in detail below. Finally, it should be noted that the width of the rovibrational lines of CO_2 at 100 Torr of pressure is ∼0.5 Å and is beyond the resolution of the spectrometer used for these measurements.

By performing frequency-resolved measurements of nonlinear focusing for strong absorption lines, we have observed intensity-dependent absorption that is consistent with power broadening. Indeed, we expect that the resonant ac-Stark effect should play a major role in this experiment since the 4.3-μm (000-001) transitions of CO_2 have a relatively large dipole moment of ∼0.3 D [20]. This effect causes the rovibrational line to broaden and, eventually, split as the applied field strength is increased, the degree of which scales in proportion to the Rabi frequency, $\Omega_R = 2\pi\mu E/h$, where μ is the dipole moment of the transition, E is the electric field strength, and h is Planck's constant. For our experimental conditions, we calculate a maximum frequency of ∼15 GHz that is much larger than the ∼300-MHz width of rovibrational lines of CO_2 at 100-Torr pressure. Figure 5(a) shows a frequency-resolved self-focusing measurement where the power broadening effect manifests as an intensity ring. The radius of the ring results from a relative increase in absorption caused by the broadening of the rovibrational line that is largest on axis where the intensity is maximum. Figure 5(b) shows the calculated CO_2 absorption spectrum in the vicinity of the $4P(30)$ (∼4305-nm) line at 100-Torr pressure and 295 K [13], where the dashed line depicts the anticipated degree of splitting based on the calculated Rabi frequency. It should be noted that the distance between rovibrational lines with a high rotational quantum number J is ∼60 GHz.

Measurements of the self-focused or self-defocused temporal pulse profile indicate that the medium has a nonlinear response time $\leqslant$4 ns FWHM. Figure 6 summarizes the results of these measurements and shows the spatial beam profile and temporal pulse profile of the initial beam [Figs. 6(a) and 6(d)] and the beam for cases when the laser was tuned to the self-focusing [Figs. 6(b) and 6(e)] and self-defocusing [Figs. 6(c) and 6(f)] sides of resonance. As can be inferred from Fig. 6(d), the initial pulse, as measured by a fast HgCdTe detector, was comprised of a ∼4-ns spike followed by a ∼30-ns tail. When the laser was tuned to the self-focusing [Figs. 6(b) and 6(e)] side of resonance only the initial 4-ns-long spike

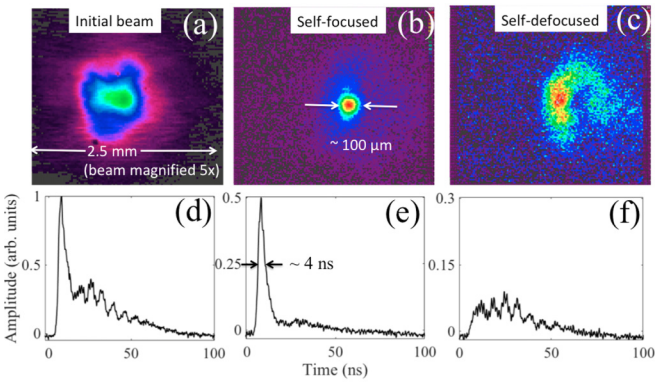

FIG. 6. Beam profile measurements of (a) the initial beam, (b) the self-focused beam, and (c) self-defocused beam that correspond to temporal pulse profile measurements (d)–(f), respectively. Note that pulse consisted of a 4-ns FWHM spike followed by a 30-ns tail and that only the initial spike was subjected to nonlinear focusing. Note that the vertical axes of (d)–(f) are normalized to the peak amplitude of the initial laser pulse. These measurements were performed in the vicinity of the $4P(30)$ line where the absorption was ~50% for (b), (e) and ~70% for (c), (f).

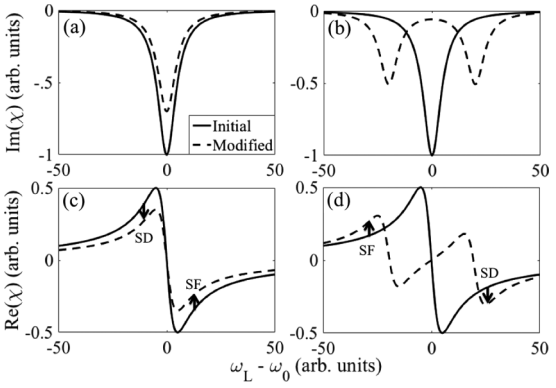

FIG. 7. Imaginary and real parts of the susceptibility (χ) when modified by (a), (c) saturation and (b), (d) power broadening, respectively. Note that ω_L-ω_0 is the detuning where ω_L is the laser frequency and ω_0 is the resonant frequency. SF and SD denote regions of self-focusing and self-defocusing, respectively.

was self-focused by the CO_2 cell and subsequently detected by the on-axis detector. When the laser was tuned on the self-defocusing side [Figs. 6(c) and 6(f)] of the resonance, the 4-ns-long spike was defocused and the on-axis detector detected only the long tail.

Finally, we estimated the nonlinear refractive index of CO_2 near the $4P(28)$ and $4P(30)$ lines of the 000-001 band of CO_2. By using a Gaussian beam decomposition method [11,21] we have fit our data using an analytic expression derived to calculate the change in beam radius of a Gaussian beam after it is subjected to a nonlinear phase shift. The value we have calculated for the nonlinear refractive index is $\sim 10^{-12}$ cm^2/W for 100 Torr of CO_2 corresponding to a critical power for Kerr self-focusing of ~10 kW. This value is consistent with our estimation of the critical power for self-focusing obtained by observing the transition from a single to multiple filamentation regime [see Fig. 2(d)]. Using a concentration of 400 ppm of CO_2 in air, we estimate that the critical power for self-focusing of 4.3-μm radiation in the atmosphere is approximately 10 MW, $\sim 10^4$ times less than the value calculated using measurements of the nonresonant nonlinear refractive index in the mid- and LWIR range, $\sim 10^{-19}$ cm^2/W [15–18].

IV. DISCUSSION

The most interesting finding of this experimental study is the sign reversal of the nonlinearity of CO_2 as compared to that of a saturable two-level system (i.e., n_2 is negative at high frequencies and positive at low frequencies relative to the rovibrational line center). This is a report of a reversal in the dispersion of the Kerr nonlinearity in either atomic or molecular gases. To understand how this nonlinearity can manifest it is useful to review the sign of the nonlinearity of a saturable, two-level system [14]. Figures 7(a) and 7(c) show the imaginary and real part of a Lorentzian line-shape function that has decreased in amplitude due to saturation. For this system, the resonant nonlinearity results in self-focusing and self-defocusing on the high- and low-frequency side of resonance, respectively [see Fig. 7(c)]. The CO_2 molecule, however, cannot be approximated as a saturable two-level system due to the existence of higher vibrational levels that are slightly detuned due to small anharmonicity and because of its rotational structure [see Fig. 1(b) and the inset of Fig. 1]. These differences make the 4.3-μm absorption channel difficult to saturate [22], particularly at the intensities used in this experiment. Indeed, it has been reported that the absorption of similar simple molecules such as SO_2, OCS, NO_2, and O_3 will not saturate even at intensities of 10^9–10^{11} W/cm^2 since power broadening can cause adjacent rovibrational lines to overlap resulting in absorption by a large number of quasiresonant rovibrational transitions [23].

Since the 4.3-μm absorption channel is not saturable, other effects must be responsible for the observed optical nonlinearity. An increase in absorption as a function of intensity can certainly lead to the qualitative behavior that is observed in experiment, and this may be possible since the excitation of population from 000 to 001 opens an absorption channel from 001 to 002. It is unlikely that this factor is responsible for our observations, however, since we observe the same sign of nonlinearity over a wide range of rovibrational lines across both the $4P$ and $4R$ branches. Figure 8 shows calculated CO_2 absorption spectra for unexcited and excited CO_2 that correspond to vibrational temperatures (T_3) of 295 K [$T_3 = T$, Fig. 8(a)] and 2500 K [$T_3 \neq T$, Fig. 8(b)], respectively. Here, we have only shown lines that correspond to the 000-001 (blue solid line) and 001-002 (red dashed line) transitions. As can be inferred from Fig. 8(b), the 001-002 transitions only coincide with the 000-001 transitions for the $4P$ branch. It should be noted that vibrational temperatures of 2500 K have been measured for an optically pumped CO_2 laser under similar experimental conditions [22].

A more likely explanation for our experimental observations is that the nonlinearity is dominated by power broadening, as our calculations of the Rabi frequency and measurements of frequency-resolved self-focusing [see Fig. 5(a)] indicate that this effect plays a major role in the experiment. To explain the qualitative sign of the nonlinearity we have used

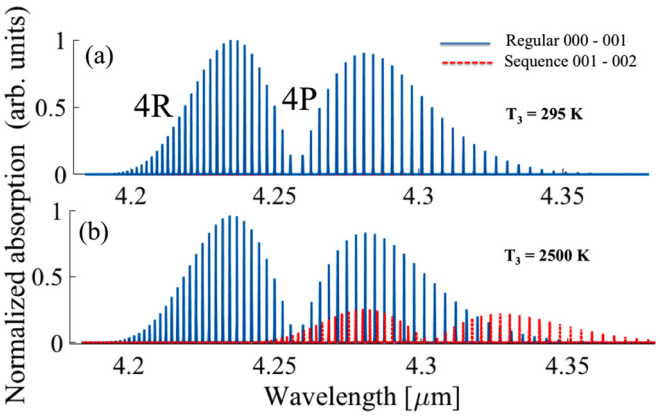

FIG. 8. Calculated absorption spectra showing lines corresponding to the 000-001 and 001-002 transitions of the CO_2 molecule for a vibrational temperature of (a) 295 K and (b) 2500 K.

a simplified model of the power broadening process where we have approximated the level splitting by a summation of two Lorentzian line-shape functions that are separated by the Rabi frequency. Figures 7(b) and 7(d) show the imaginary and real part of this function, respectively, where the degree of level splitting is comparable to that expected for our experimental conditions. As can be seen from Fig. 7(d), this level splitting may cause self-focusing on the low-frequency and self-defocusing on the high-frequency wing of the absorption line, consistent with what has been observed in experiment. Figure 7(d) also suggests that the nonlinearity changes sign within the bandwidth of the unperturbed resonant line. This fine structure was not observed in experiment, due to limitations in this simplified model or for experimental reasons such as high absorption or insufficient resolution.

The time-domain data presented in Fig. 6, suggesting that the nonlinear response time is <4 ns, are consistent with the instantaneous response time that is expected from a field effect such as power broadening. A nonlinear response originating from excitation, on the other hand, should respond on a timescale related to the upper state lifetime, $\sim 40\,\mu$s for the 100-Torr pressures used in our experiment [24,25]. While this finding suggests that power broadening is the dominant mechanism in this experiment, the resonant nonlinear optics of simple molecules such as CO_2 are complicated by a combination of excitation and power broadening effects. A comparison between high-resolution spectral measurements and calculations using a self-consistent, density-matrix approach is necessary to completely elucidate the physics.

V. CONCLUSIONS

We have used time- and frequency-resolved measurements of self-focusing and self-defocusing to characterize the resonant rovibrational nonlinear optical response of the CO_2 molecule at $4.3\,\mu$m. In doing so, we have performed measurements of the qualitative dispersion of the resonant nonlinearity in the vicinity of individual rovibrational lines. When subjected to intense 4.3-μm laser pulses, the CO_2 molecule exhibits a nonlinearity which is opposite in sign to that predicted by the two-level model and that observed in other atomic and molecular gases, thus underscoring the importance of performing such measurements for a number of simple molecules. The data suggest that, owing to the relatively large dipole moment of the asymmetric stretching mode of CO_2, power broadening and level splitting dominates the nonlinear response. Future work will be dedicated to performing a detailed comparison between high-resolution measurements and theory to fully understand the physics of this resonant rovibrational nonlinearity. These measurements are directly applicable to the development of optically pumped molecular lasers and could prove useful for establishing a nonlinear refractive index equivalent of the HITRAN database, a task that is critical to support research on the propagation of high-power mid- and LWIR beams in the atmosphere.

ACKNOWLEDGMENTS

This material is based upon work supported by the Office of Naval Research (ONR) MURI (4-442521-JC-22891) and the Department of Energy (DOE) Office of Science Accelerator Stewardship Award No. DE-SC0018378.

[1] S. L. McCall and E. L. Hahn, Self-Induced Transparency by Pulsed Coherent Light, Phys. Rev. Lett. **18**, 908 (1967).

[2] D. Grischkowsky, Self-Focusing of Light by Potassium Vapor, Phys. Rev. Lett. **24**, 866 (1970).

[3] D. Grischkowsky and J. A. Armstrong, Self-defocusing of light by adiabatic following in rubidium vapor, Phys. Rev. A **6**, 1566 (1972).

[4] K.-J. Boller, A. Imamoğlu, and S. E. Harris, Observation of Electromagnetically Induced Transparency, Phys. Rev. Lett. **66**, 2593 (1991).

[5] A. Kasapi, M. Jain, G. Y. Yin, and S. E. Harris, Electromagnetically Induced Transparency: Propagation Dynamics, Phys. Rev. Lett. **74**, 2447 (1995).

[6] M. D. Lukin and A. Imamoğlu, Nonlinear Optics and Quantum Entanglement of Ultraslow Single Photons, Phys. Rev. Lett. **84**, 1419 (2000).

[7] P. Bernard, P. Galarneau, and S. L. Chin, Self-focusing of CO_2 laser pulses in low-pressure SF_6, Opt. Lett. **6**, 139 (1981).

[8] I. A. Al-Saidi, D. J. Biswas, C. A. Emshary, and R. G. Harrison, Self focussing of CO_2 laser radiation in NH_3 gas, Opt. Commun. **52**, 336 (1985).

[9] B. K. Deka, R. S. Joshi, and M. A. Rob, Self-focusing and defocusing of TEA CO_2 laser radiation in NH_3, Appl. Phys. B **44**, 1 (1987).

[10] Y. Beaudoin, P. Galarneau, A. Normandin, and S. L. Chin, An experimental study of self-focusing and self-defocusing of a TEA CO_2 laser pulse in CDF_3, Appl. Phys. B **42**, 225 (1987).

[11] C. H. Oh and S. S. Lee, Measurement of nonlinear refractive index coefficients of NH_3 gas for transversely excited atmospheric CO_2 laser lines, J. Appl. Phys. **65**, 276 (1989).

[12] S. Tochitsky, E. Welch, M. Polyanskiy, I. Pogorelsky, P. Panagiotopoulos, M. Kolesik, E. M. Wright, S. W. Koch, J. V. Moloney, J. Pigeon, and C. Joshi, Megafilament in air formed

by a self-guided terawatt long-wavelength infrared laser. Nat. Photonics **13**, 41 (2019).

[13] I. E. Gordon, L. S. Rothman, and C. Hill *et al.*, The HITRAN2016 molecular spectroscopic database, J. Quant. Spectrosc. Radiat. Transfer **203**, 3 (2017).

[14] A. Javan and P. L. Kelley, Possibility of self-focusing due to intensity dependent anomalous dispersion, IEEE J. Quantum Electron. **2**, 470 (1966).

[15] S. Zahedpour, J. K. Wahlstrand, and H. M. Milchberg, Measurement of the nonlinear refractive index of air constituents at mid-infrared wavelengths, Opt. Lett. **40**, 5794 (2015).

[16] J. J. Pigeon, S. Ya. Tochitsky, E. C. Welch, and C. Joshi, Measurements of the nonlinear refractive index of air, N_2, and O_2 at 10 μm using four-wave mixing, Opt. Lett. **41**, 3924 (2016).

[17] J. J. Pigeon, S. Ya. Tochitsky, E. C. Welch, and C. Joshi, Experimental study of the third-order nonlinearity of atomic and molecular gases using 10-μm laser pulses, Phys. Rev. A **97**, 043829 (2018).

[18] S. Zahedpour, S. W. Hancock, and H. M. Milchberg, Ultrashort infrared 2.5–11 μm pulses: spatiotemporal profiles and absolute nonlinear response of air constituents, Opt. Lett. **44**, 843 (2019).

[19] V. Fedorov, D. Martyshkin, K. Karki, and S. Mirov, Gain switched and *Q*-switched Fe:ZnSe lasers tunable over 3.60–5.15 μm, in *Laser Congress 2018 (ASSL)*, OSA Technical Digest (Optical Society of America, Washington, D.C., 2018), paper AW3A.6.

[20] R. K. Brimacombe and J. Reid, Influence of the dynamic Stark effect on the small-signal gain of optically pumped 4.3-μm CO_2 lasers, J. Appl. Phys. **58**, 1141 (1985).

[21] D. Weaire, B. S. Wherrett, D. A. B. Miller, and S. D. Smith, Effect of low-power nonlinear refraction on laser-beam propagation in InSb, Opt. Lett. **4**, 331 (1979).

[22] R. C. Y. Auyeung and J. Reid, High Vibrational temperatures in optically-pumped CO_2, IEEE J. Quantum Electron. **24**, 573 (1988).

[23] A. V. Chugunov, M. S. Djidjoev, S. V. Ivanov, and V. Ya. Panchenko, Nonlinear absorption of strong infrared radiation by ozone, Opt. Lett. **10**, 615 (1985).

[24] F. Lepoutre, G. Louis, and H. Manceau, Collisional relaxation in CO_2 between 180 K and 400 K measured by the spectrophone method, Chem. Phys. Lett. **48**, 509 (1977).

[25] G. Inoue and S. Tsuchiya, Vibrational relaxation of $CO_2(00^01)$ in CO_2, He, Ne, and Ar in the temperature range from 300 $\sim$ 140 K, J. Phys. Soc. Jpn. **38**, 870 (1975).